ELSEVIER

Journal of Organometallic Chemistry 544 (1997) 189–196

Journal of Organometallic Chemistry

Organometallic complexes for non-linear optics XII [1] Syntheses and second-order susceptibilities of (neomenthyldiphenylphosphine)gold σ-arylacetylides: X-ray crystal structures of Au(C≡CPh)(nmdpp) and Au((*E*)-4,4′-C≡CC$_6$H$_4$CH=CHC$_6$H$_4$NO$_2$)(nmdpp)

Ian R. Whittall [a], Mark G. Humphrey [a,*], Marek Samoc [b], Barry Luther-Davies [b], David C.R. Hockless [c]

[a] *Department of Chemistry, Australian National University, Canberra, ACT 0200, Australia*

[b] *Australian Photonics Cooperative Research Centre, Laser Physics Centre, Research School of Physical Sciences and Engineering, Australian National University, Canberra, ACT 0200, Australia*

[c] *Research School of Chemistry, Australian National University, Canberra, ACT 0200, Australia*

Received 16 January 1997

Abstract

The series of complexes Au(C≡CR)(nmdpp) (R = Ph (**2**), 4-C$_6$H$_4$NO$_2$ (**3**), 4,4′-C$_6$H$_4$C$_6$H$_4$NO$_2$ (**4**), (*E*)-4,4′-C$_6$H$_4$CH=CHC$_6$H$_4$NO$_2$ (**5**), (*Z*)-4,4′-C$_6$H$_4$CH=CHC$_6$H$_4$NO$_2$ (**6**), 4,4′-C$_6$H$_4$C≡CC$_6$H$_4$NO$_2$ (**7**), 4,4′-C$_6$H$_4$N=CHC$_6$H$_4$NO$_2$ (**8**); nmdpp = (+)-neomenthyldiphenylphosphine) has been synthesized by reaction of AuCl(nmdpp) with the corresponding acetylene and methoxide in the presence of trace amounts of a phosphine oxide, and complexes **2** and **5** have been structurally characterized. Complexes **2**–**8** and analogous (triphenylphosphine)gold acetylides and precursor (phosphine)gold chlorides have been examined for their second-order bulk susceptibilities $\chi^{(2)}$ by the Kurtz powder technique, with the largest response (ca. 2 × urea) being that from **3**. © 1997 Elsevier Science S.A.

Keywords: Gold; Chiral; Acetylide; Alkynyl; Susceptibility; Kurtz

1. Introduction

The non-linear optical (NLO) properties of organometallic complexes are of great current interest [2–5]. Our investigations in this field have focused on metal acetylide complexes; they are usually thermally robust, oxidatively stable, and accessible in high yield by established synthetic methodologies. We have concentrated thus far on molecular measurements, and have utilized electric-field-induced second harmonic generation and hyper-Rayleigh scattering to probe second-order non-linearities [1,6–9], ZINDO [10] to compute second-order non-linearities [6,8,11–13], and Z-scan and degenerate four-wave mixing to determine third-order non-linearities [1,8,14–16]. Bulk material NLO responses are of importance to assess potential in various device applications, but we have not until now evaluated the macroscopic quadratic NLO merit of acetylide complexes. We report herein syntheses of (phosphine)gold acetylide complexes incorporating the chiral phosphine (+)-neomenthyldiphenylphosphine (nmdpp), X-ray crystal structures of two examples, and Kurtz powder measurements of their efficiency at (second harmonic generation SHG), together with similar data for the previously-reported (triphenylphosphine)gold acetylide analogues and precursor (phosphine)gold chlorides.

2. Results and discussion

2.1. Syntheses and characterization of gold complexes

AuCl(nmdpp) was prepared by adapting the literature synthesis, where tetrachloroauric acid is reduced by

* Corresponding author. E-mail: Mark.Humphrey@anu.edu.au.

[1] For Part XI, see Ref. [1].

PII S0022-328X(97)00196-4

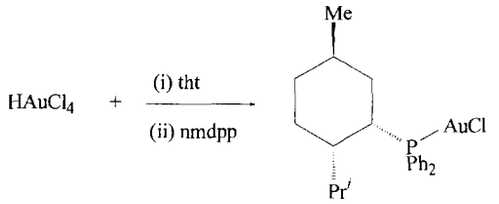

Scheme 1.

tetrahydrothiophene (tht) [17] and the tht-stabilized product AuCl(tht) is subsequently reacted with one equivalent of phosphine. This procedure avoids consumption of phosphine in the reduction of Au^{III} to Au^{I} in, for example, the preparation of (triphenylphosphine)gold chloride from direct reaction between $HAuCl_4$ and PPh_3 [18], an important consideration when utilizing an expensive phosphine. Following this procedure, AuCl(tht) was reacted with one equivalent of nmdpp at room temperature to afford AuCl(nmdpp) (**1**) as a colourless complex (Scheme 1). Complex **1** was identified by ^1H and ^{31}P NMR, UV–vis spectroscopies, mass spectrometry and satisfactory microanalyses.

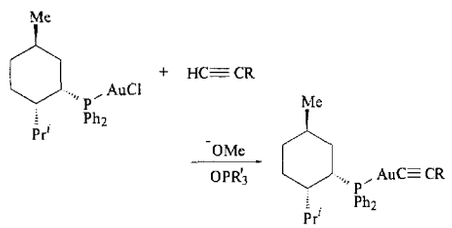

Complex	R	% Yield
2	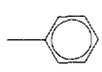	47
3	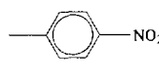	69
4	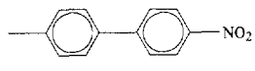	65
5	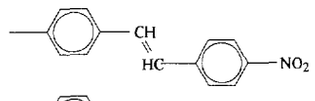	61
6	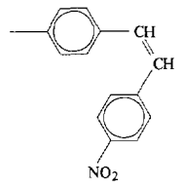	78
7	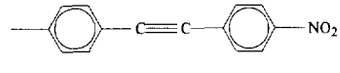	71
8	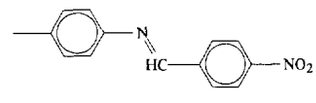	53

Scheme 2.

The new acetylide complexes were prepared in good to excellent yields (47–78%) by extension of literature procedures [7,19,20], or modifications thereof (Scheme 2). Complexes **2–8** were characterized by IR, ^1H and ^{31}P NMR spectroscopies, mass spectrometry, and satisfactory microanalyses. For **2–8**, characteristic $\nu(C{\equiv}C)$ in the solution IR spectra are found between 2113 and 2116 cm^{-1}; as $\nu(C{\equiv}C)$ was found in the range 2112–2116 cm^{-1} for the analogous series of (triphenylphosphine)gold acetylide complexes [7], this parameter is insensitive to variation in the phosphine. For **2–8**, phosphine P in the ^{31}P NMR are insensitive to acetylide variation, being found between 38.5 and 38.6 ppm. The mass spectra for **2–8** all show peaks corresponding to protonation of the molecular ion and fragmentation by loss of acetylide, together with peaks assigned to (phosphine)auration of the molecular ion and $[Au(nmdpp)_2]^+$. The UV–visible spectra for complexes **3–8** are characterized by intense (ε = 15 000–39 000 M^{-1} cm^{-1}) MLCT bands at lowest frequency together with higher energy bands assigned to $\sigma(Au \leftarrow P) \rightarrow \pi^*(PPh)$. Replacement of aryl 4-H by 4-NO_2 in the phenylacetylide ligand in proceeding from **2** to **3** results in a red shift of 46 nm in λ_{max}; a similar replacement for Au(4-$C{\equiv}CC_6H_4R$)(PPh_3) (R = H, NO_2) resulted in a 42 nm shift to lower energy [7]. Chain lengthening of the acetylide chromophore leads, as expected, to a bathochromic shift of the MLCT band, with **5** and **8** containing the lowest energy transitions.

2.2. X-ray structural studies

We have completed X-ray diffraction studies on complexes **2** and **5**. Both complexes **2** and **5** contain

Table 1
Crystallographic data for complexes **2** and **5**

	2	**5**
Empirical formula	$C_{30}H_{34}AuP$	$C_{38}H_{18}AuNO_2P$
Molecular weight	622.5	748.5
Crystal colour, habit	colourless, block	yellow, block
Crystal dimensions (mm^3)	0.2×0.4×0.4	0.3×0.3×0.2
Space group	$P2_1$ (#4)	$P\bar{1}$ (#2)
a (Å)	10.187(7)	12.833(1)
b (Å)	17.355(2)	15.422(2)
c (Å)	15.461(2)	19.052(2)
α (deg)		71.848(9)
β (deg)	102.36(2)	80.551(9)
γ (deg)		73.884(8)
V ($Å^3$)	2670(1)	3429.5(7)
Z	4	4
D_{calc} ($g cm^{-3}$)	1.55	1.45
Trans. factors	0.28–1.00	0.82–1.00
N	4900	10200
N_0 ($I > 3.00\sigma(I)$)	4048	7551
No. variables	576	732
p-factor	0.001	0.020
R	0.033	0.073
R_w	0.023	0.087

Table 2
Important geometric parameters for Au(C≡CPh)(nmdpp) (**2**)

	2A	2B		2A	2B
Au(1)–P(1)	2.296(4)	2.292(3)	C(3)–C(4)	1.37(2)	1.36(2)
Au(1)–C(1)	2.00(1)	2.00(2)	C(3)–C(8)	1.40(2)	1.34(2)
P(1)–C(111)	1.93(1)	1.85(1)	C(4)–C(5)	1.33(2)	1.38(2)
P(1)–C(121)	1.86(1)	1.83(1)	C(5)–C(6)	1.33(2)	1.33(2)
P(1)–C(131)	1.87(1)	1.88(1)	C(6)–C(7)	1.40(2)	1.31(3)
C(1)–C(2)	1.21(2)	1.21(2)	C(7)–C(8)	1.40(2)	1.42(2)
C(2)–C(3)	1.46(2)	1.42(2)			
P(1)–Au(1)–C(1)	179.6(4)	177.3(4)	C(2)–C(3)–C(4)	122(1)	121(1)
Au(1)–P(1)–C(111)	116.6(5)	117.3(4)	C(2)–C(3)–C(8)	117(1)	122(1)
Au(1)–P(1)–C(121)	111.1(5)	113.9(5)	C(4)–C(3)–C8)	120(1)	117(1)
Au(1)–P(1)–C(131)	110.4(4)	108.5(4)	C(3)–C(4)–C(5)	120(2)	122(1)
C(111)–P(1)–C(121)	106.7(7)	104.0(7)	C(4)–C(5)–C(6)	123(2)	122(2)
C(111)–P(1)–C(131)	106.9(6)	109.4(6)	C(5)–C(6)–C(7)	119(2)	117(2)
C(121)–P(1)–C(131)	104.4(6)	102.7(6)	C(6)–C(7)–C(8)	119(2)	124(2)
Au(1)–C(1)–C(2)	176(1)	175(1)	C(3)–C(8)–C(7)	118(1)	119(2)
C(1)–C(2)–C(3)	176(2)	176(2)			

two independent molecules in the asymmetric unit, neither of which differs in bond length and angle data within the error margins. Problems associated with pseudosymmetry have necessitated a cautious exposition of the crystal structure of **5**; the determination is sufficient to confirm the atom connectivity and molecular disposition in the crystal lattice, and subsequent discussion of **5** is restricted to these considerations. Crystallographic data are collected in Table 1 and important geometric parameters for **2** are shown in Table 2. ORTEP plots of one independent molecule of both **2** and **5** are displayed in Fig. 1 (**2**) and Fig. 2 (**5**).

The structural study of **2** confirms the molecular composition inferred from spectral data. It is the first (nmdpp)gold complex to be structurally characterized, although examples of this ligand attached to chromium [21], iron [22], ruthenium [23], and platinum [24] have appeared. The Au–P(1) distance (2.296(4), 2.292(3) Å) is similar to that in other (phosphine)gold complexes (e.g. 2.277(1) Å in Au(4-C≡C$C_6H_4NO_2$)(PPh_3) [7]), and intraphosphine bond lengths and angles are unexceptional. The P(1)–Au–C(1) (179.6(4)°) and Au–C(1)–C(2) (176(1)°) angles are close to linearity as expected, and the arylacetylide distances and angles are within the range of those previously observed (for a comprehensive listing of relevant data from previous (phosphine)gold acetylide structural studies see Ref. [7]); complex **2** is the first structural study of a gold acetylide incorporating a chiral phosphine ligand. Almost half the previous (phosphine)gold acetylide X-ray structural analyses have revealed a short Au · · · Au contact believed to result from a weak relativistic bonding force, one example being Au(C≡CPh)(PPh_3) (Au · · · Au 3.379(1) Å). It is interesting that replacing phenyl by neomenthyl in proceeding to **2** modifies the steric interactions so as to disfavour a short Au · · · Au contact (no Au · · · Au interaction exists in the crystal lattice of **2** within an intermolecular separation of 5 Å).

The most interesting feature of the structural studies of **2** and **5** is the molecular disposition in the crystal

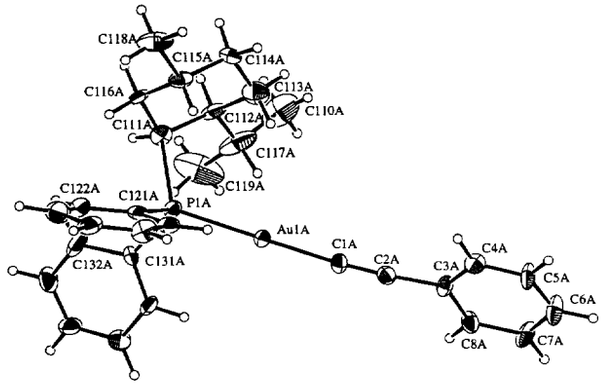

Fig. 1. Molecular structure and atomic labelling scheme for one of the molecules of Au(C≡CPh)(nmdpp) (**2**). 20% thermal ellipsoids are shown for the non-hydrogen atoms; hydrogen atoms have arbitrary radii.

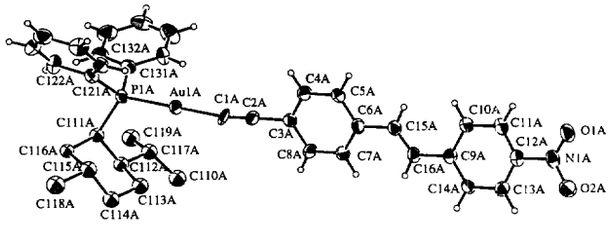

Fig. 2. Molecular structure and atomic labelling scheme for one of the molecules of Au((*E*)-4,4′-C≡CC_6H_4CH=CH$C_6H_4NO_2$)(nmdpp) (**5**). 20% thermal ellipsoids are shown for the non-hydrogen atoms; hydrogen atoms have arbitrary radii.

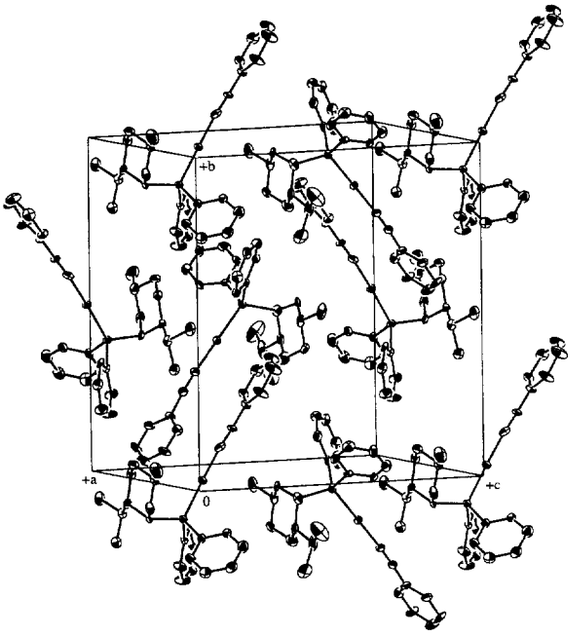

Fig. 3. Cell packing diagram of Au(C≡CPh)(nmdpp) (**2**).

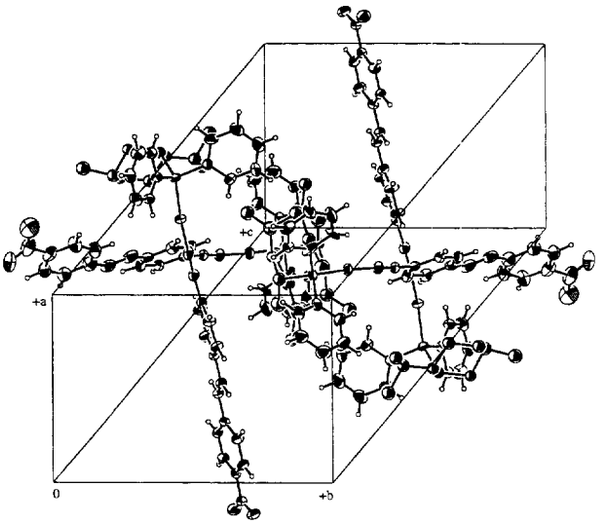

Fig. 4. Cell packing diagram of Au((*E*)-4,4′-C≡CC$_6$H$_4$CH=CHC$_6$H$_4$NO$_2$)(nmdpp) (**5**).

lattice. With this in mind, the cell packing for both **2** and **5** has been investigated, and is displayed in Fig. 3 (**2**) and Fig. 4 (**5**). With **5**, the molecular dipole is opposed to that of an adjacent molecule. A similar antiparallel arrangement of phenylacetylide groups is found in the crystal structure of **2**. Although incorporation of chiral ligands has been suggested as one route to enforce favourable molecular alignment required to translate large molecular non-linearities into large bulk susceptibilities, the driving force for opposing dipoles in donor–acceptor molecules such as **5** is sufficiently great as to limit the usefulness of this strategy. Even examples such as **2**, which do not have a large ground state dipole, can pack such that the metal–alkynyl groups adopt antiparallel arrangements on adjacent molecules.

2.3. Powder SHG measurements

The powder SHG and responses of complexes **1–8**, together with those of their triphenylphosphine analogues, were measured by the Kurtz method [25] and are listed in Table 3.

Significantly, all four (phosphine)gold chlorides and phenylacetylides which lack a strong donor–bridge–acceptor composition gave zero responses. All ten compounds of the 'extended chain' acetylide ligands decomposed with fluorescence (this fluorescence is likely to be a result of multiphoton, particularly two-photon, absorption). It is significant that when carrying out hyper-Rayleigh scattering measurements to determine molecular non-linearities of the (triphenylphosphine)gold acetylide complexes, we noted

Table 3
Bulk second-order responses by the Kurtz powder technique

Complex	Powder response (urea = 1)
AuCl(nmdpp) (**1**)	0
Au(C≡CPh)(nmdpp) (**2**)	0
Au(4-C≡CC$_6$H$_4$NO$_2$)(nmdpp) (**3**)	2
Au(4,4′-C≡CC$_6$H$_4$C$_6$H$_4$NO$_2$)(nmdpp) (**4**)	< 1 fluoresced, decomposed
Au((*E*)-4,4′-C≡CC$_6$H$_4$CH=CHC$_6$H$_4$NO$_2$)(nmdpp) (**5**)	< 1 fluoresced, decomposed
Au((*Z*)-4,4′-C≡CC$_6$H$_4$CH=CHC$_6$H$_4$NO$_2$)(nmdpp) (**6**)	< 1 fluoresced, decomposed
Au(4,4′-C≡CC$_6$H$_4$C≡CC$_6$H$_4$NO$_2$)(nmdpp) (**7**)	< 1 fluoresced, decomposed
Au(4,4′-C≡CC$_6$H$_4$N=CHC$_6$H$_4$NO$_2$)(nmdpp) (**8**)	< 1 fluoresced, decomposed
AuCl(PPh$_3$)	0
Au(C≡CPh)(PPh$_3$)	0
Au(4-C≡CC$_6$H$_4$NO$_2$)(PPh$_3$)	0
Au(4,4′-C≡CC$_6$H$_4$C$_6$H$_4$NO$_2$)(PPh$_3$)	fluoresced, decomposed
Au((*E*)-4,4′-C≡CC$_6$H$_4$CH=CHC$_6$H$_4$NO$_2$)(PPh$_3$)	fluoresced, decomposed
Au((*Z*)-4,4′-C≡CC$_6$H$_4$CH=CHC$_6$H$_4$NO$_2$)(PPh$_3$)	fluoresced, decomposed
Au(4,4′-C≡CC$_6$H$_4$C≡CC$_6$H$_4$NO$_2$)(PPh$_3$)	fluoresced, decomposed
Au(4,4′-C≡CC$_6$H$_4$N=CHC$_6$H$_4$NO$_2$)(PPh$_3$)	fluoresced, decomposed

strong fluorescence of Au((*Z*)-4,4′-C≡CC$_6$H$_4$CH=CHC$_6$H$_4$NO$_2$)(PPh$_3$); see Ref. [7]. The 4-nitrophenylacetylide complexes were stable to irradiation by the laser, with only the nmdpp example producing a measurable bulk non-linearity (2 × urea). Molecular NLO measurements of (cyclopentadienyl)bis(phosphine)ruthenium acetylide complexes revealed a small decrease in non-linearity upon replacing triphenylphosphine by trimethylphosphine [11], so replacing triphenylphosphine by nmdpp would not be expected to increase the molecular non-linearity; it is likely, therefore, that favourable molecular alignment not observed with the triphenylphosphine analogue is responsible for the significant bulk non-linearity for complex **3**. Complex Au(4-C≡CC$_6$H$_4$NO$_2$)(PPh$_3$) crystallizes in the centrosymmetric space group $P2_1/c$ [7], but the lack of an X-ray structural study of **3** and consequent crystal packing information precludes anything more than this cautious comment. Although chiral ligand introduction has been successful in the present work in affording the enhanced non-linearity of **3** compared to that of its triphenylphosphine analogue, the cell packing of both **2** and **5** shows that this strategy is somewhat 'hit or miss' as it suffers from lack of control over the molecular disposition in the crystal. Further studies of the NLO responses of organometallic complexes are currently underway.

3. Experimental section

3.1. General conditions

All organometallic reactions were carried out under an atmosphere of nitrogen with the use of standard Schlenk techniques; no attempt was made to exclude air during work-up of organometallic products. Phenylacetylene (Aldrich), tht and chloroauric acid (BDH) were used as-received; nmdpp [26], 4-HC≡CC$_6$H$_4$NO$_2$ [27], 4,4′-HC≡CC$_6$H$_4$C$_6$H$_4$NO$_2$ [8], (*E*)- and (*Z*)-4,4′-HC≡CC$_6$H$_4$CH=CHC$_6$H$_4$NO$_2$ [28], 4,4′-HC≡CC$_6$H$_4$C≡CC$_6$H$_4$NO$_2$ [8] and 4,4′-HC≡CC$_6$H$_4$N=CHC$_6$H$_4$NO$_2$ [6] were prepared following the literature methods. Triphenylphosphine oxide and nmdpp oxide are the by-products of the reaction of two equivalents of the corresponding phosphine with chloroauric acid. Mass spectra were recorded using a VG ZAB 2SEQ instrument (30 kV Cs$^+$ ions, current 1 mA, accelerating potential 8 kV, 3-nitrobenzyl alcohol matrix) at the Research School of Chemistry, Australian National University; peaks are reported as *m/z* (assignment, relative intensity). Microanalyses were carried out at the Research School of Chemistry, Australian National University. Infrared spectra were recorded using a Perkin–Elmer System 2000 FT-IR spectrometer. UV–visible spectra were recorded using a Cary 5 spectrophotometer. ^{1}H and ^{31}P NMR spectra were recorded using a Varian Gemini-300 FT NMR spectrometer and are referenced to residual CHCl$_3$ (7.24 ppm) or external 85% H$_3$PO$_4$ (0.0 ppm), respectively. Spectral assignments follow the numbering scheme shown in Fig. 5.

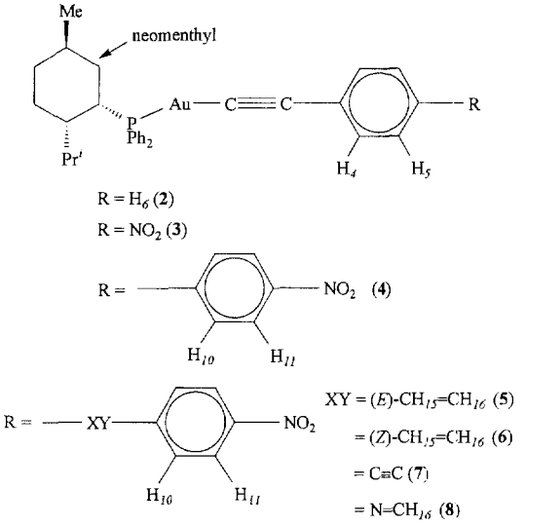

Fig. 5. Numbering scheme for NMR spectral assignment.

3.2. Syntheses of (nmdpp)gold acetylides

3.2.1. Synthesis of AuCl(nmdpp) (1)

The complex AuCl(nmdpp) (**1**) was prepared by a modification to the literature procedure [17]. The dropwise addition of tht to an ethanol solution of HAuCl$_4$ · ~ 3H$_2$O (1 g in 10 ml) caused a white solid to precipitate; addition of tht was continued until no further precipitate formed. The precipitated AuCl(tht) was collected by filtration (0.76 g, 93% based on HAuCl$_4$ · 3H$_2$O). AuCl(tht) (0.76 g, 2.37 mmol) and (+)-nmdpp (0.78 g, 2.40 mmol) were stirred together in acetone (10 ml) for 10 min at room temperature. The solvent volume was reduced, whereupon the white product AuCl(nmdpp) (**1**) precipitated and was collected by filtration and washed with ether (0.98 g, 74%). (A further 200 mg (15%) of slightly lower quality could be collected by reducing the filtrate to dryness.) Anal. Calc. for C$_{22}$H$_{29}$AuClP: C 47.45, H 5.25%. Found: C 47.54, H 5.36%. ^{1}H NMR: (δ, 300 MHz, CDCl$_3$); (0.49 (d, J_{HH} = 6 Hz, 3H), 0.58 (d, J_{HH} = 6 Hz, 3H), 0.76 (d, J_{HH} = 6 Hz, 3H), 0.97 (m), 1.32 (m), 1.63 (m), 1.92 (m), 2.08 (m), 2.80 (m), 3.50 (m), neomenthyl), (7.43 (m), 7.88 (m), 8.07 (m), Ph). ^{31}P NMR: (δ, 121 MHz, CDCl$_3$); 31.9. UV–vis: λ (nm) (ε (M^{-1} cm^{-1})) (thf): 275 (1200), 267 (1600). FAB MS; *m/z* (fragment, relative intensity): 1077 ([M + Au(nmdpp)]$^+$, 100), 845 ([Au(nmdpp)$_2$]$^+$, 22), 521 ([M − Cl]$^+$, 33), 383 ([M − Cl − neomenthyl + H]$^+$, 34).

3.2.2. Synthesis of Au(C≡CPh)(nmdpp) (2)

AuCl(nmdpp) (95 mg, 0.17 mmol), a trace of nmdpp oxide and phenylacetylene (50 mg, 0.49 mmol) were added to a methanol solution of sodium methoxide (10 ml, 0.25 M), and the resultant mixture stirred for 5 h at room temperature. The solvent volume was concentrated to 2 ml, affording the product as a white powder (50 mg, 47%). Anal. Calc. for $C_{30}H_{34}AuP$: C 57.87, H 5.52%. Found: C 57.84, H 5.74%. IR: (CH_2Cl_2) ν(C≡C) 2115 (vw) cm^{-1}. ^1H NMR: (δ, 300 MHz, $CDCl_3$); (0.48 (d, J_{HH} = 6 Hz, 3H), 0.57 (d, J_{HH} = 6 Hz, 3H), 0.76 (d, J_{HH} = 6 Hz, 3H), 0.95 (m), 1.30 (m), 1.60 (m), 1.96 (m), 2.78 (m), 3.58 (m), neomenthyl), (7.40 (m), 7.93 (m), 8.12 (m), Ph), 7.23 (m, H_5), H_6 is obscured, 7.55 (d, J_{HH} = 8 Hz, 2H, H_4). ^{31}P NMR: (δ, 121 MHz, $CDCl_3$); 38.6. UV–vis: λ (nm) (ε (M^{-1} cm^{-1})) (thf): 293 (11 700), 284 (33 300), 270 (30 000), 257 (16 700), 237 (28 800). FAB MS; *m/z* (fragment, relative intensity): 1144 ([M + Au(nmdpp)]$^+$, 100), 845 ([Au(nmdpp)$_2$]$^+$, 94), 623 ([M + H]$^+$, 11), 521 ([M − C≡CPh]$^+$, 17), 383 ([M − C≡CPh − neomenthyl + H]$^+$, 80), 305 ([M − C≡CPh − neomenthyl − Ph]$^+$, 20). Crystals of **2** suitable for diffraction analysis were grown by slow evaporation of acetone from a solution in acetone–hexane.

3.2.3. Synthesis of Au(4-C≡CC$_6$H$_4$NO$_2$)(nmdpp) (3)

Following the method for the preparation of **2**, AuCl(nmdpp) (140 mg, 0.25 mmol) and 4,4′-HC≡CC$_6$H$_4$NO$_2$ (50 mg, 0.34 mmol) were reacted affording Au(4-C≡CC$_6$H$_4$NO$_2$)(nmdpp) (**3**) as a pale yellow powder (50 mg, 69%). Anal. Calc. for $C_{30}H_{33}AuNO_2P$: C 53.98, H 4.98, N 2.10%. Found: C 53.86, H 4.94, N 1.97%. IR: (CH_2Cl_2) ν(C≡C) 2116 cm^{-1}. ^1H NMR: (δ, 300 MHz, $CDCl_3$); (0.49 (d, J_{HH} = 6 Hz, 3H), 0.58 (d, J_{HH} = 6 Hz, 3H), 0.77 (d, J_{HH} = 6 Hz, 3H), 0.96 (m), 1.30 (m), 1.60 (m), 1.95 (m), 2.74 (m), 3.59 (m), neomenthyl), (7.43 (m), 7.91 (m), 8.09 (m), Ph), 7.64 (d, J_{HH} = 9 Hz, 2H, H_4), 8.13 (d, J_{HH} = 9 Hz, 2H, H_5). ^{31}P NMR: (δ, 121 MHz, $CDCl_3$); 38.5. UV–vis: λ (nm) (ε (M^{-1} cm^{-1})) (thf): 339 (21 400). FAB MS; *m/z* (fragment, relative intensity): 1188 ([M + Au(nmdpp)]$^+$, 16), 845 ([Au(nmdpp)$_2$]$^+$, 100), 668 ([M + H]$^+$, 5), 521 ([M − C≡CC$_6$H$_4$NO$_2$]$^+$, 11), 383 ([M − C≡CC$_6$H$_4$NO$_2$ − neomenthyl + H]$^+$, 30), 305 ([M − C≡CC$_6$H$_4$NO$_2$ − neomenthyl − Ph]$^+$, 7).

3.2.4. Synthesis of Au(4,4′-C≡CC$_6$H$_4$C$_6$H$_4$NO$_2$)(nmdpp) (4)

AuCl(nmdpp) (50 mg, 0.09 mmol), a trace of nmdpp oxide and 4,4′-HC≡CC$_6$H$_4$C$_6$H$_4$NO$_2$ (28 mg, 0.49 mmol) were dissolved in dichloromethane (5 ml). A methanol solution of sodium methoxide (5 ml, 0.5 M) was added and the mixture was stirred for 16 h at room temperature. The solvent volume was concentrated to 4 ml affording the product as a yellow powder (42 mg, 65%). Anal. Calc. for $C_{36}H_{37}AuNO_2P$: C 58.14, H 5.03, N 1.88%. Found: C 58.45, H 5.22, N 1.83%. IR: (CH_2Cl_2) ν(C≡C) 2115 cm^{-1}. ^1H NMR: (δ, 300 MHz, $CDCl_3$); (0.48 (d, J_{HH} = 6 Hz, 3H), 0.58 (d, J_{HH} = 6 Hz, 3H), 0.75 (d, J_{HH} = 6 Hz, 3H), 0.95 (m), 1.30 (m), 1.60 (m), 1.95 (m), 2.80 (m), 3.50 (m), neomenthyl), (7.42 (m), 7.88 (m), 8.06 (m), Ph), H_4 is obscured, 7.57 (d, J_{HH} = 8 Hz, 2H, H_5), 7.72 (d, J_{HH} = 9 Hz, 2H, H_{10}), 8.28 (d, J_{HH} = 9 Hz, 2H, H_{11}). ^{31}P NMR: (δ, 121 MHz, $CDCl_3$); 38.6. UV–vis: λ (nm) (ε (M^{-1} cm^{-1})) (thf): 348 (28 700), 285 (35 100), 270 (20 500). FAB MS; *m/z* (fragment, relative intensity): 1264 ([M + Au(nmdpp)]$^+$, 58), 845 ([Au(nmdpp)$_2$]$^+$, 62), 744 ([M + H]$^+$, 32), 521 ([M − C≡CC$_6$H$_4$C$_6$H$_4$NO$_2$]$^+$, 40), 383 ([M − C≡CC$_6$H$_4$C$_6$H$_4$NO$_2$ − neomenthyl + H]$^+$, 100), 305 ([M − C≡CC$_6$H$_4$C$_6$H$_4$NO$_2$ − neomenthyl − Ph]$^+$, 20).

3.2.5. Synthesis of Au((E)-4,4′-C≡CC$_6$H$_4$CH=CHC$_6$H$_4$NO$_2$)(nmdpp) (5)

Following the method for the preparation of (**4**), AuCl(nmdpp) (50 mg, 0.09 mmol) and (*E*)-4,4′-HC≡CC$_6$H$_4$CH=CHC$_6$H$_4$NO$_2$ (22 mg, 0.09 mmol) were reacted affording Au((*E*)-4,4′-C≡CC$_6$H$_4$CH=CHC$_6$H$_4$NO$_2$)(nmdpp) (**5**) as a yellow powder (42 mg, 61%). Anal. Calc. for $C_{38}H_{39}AuNO_2P$: C 59.29, H 5.12, N 1.82%. Found: C 59.30, H 5.19, N 1.79%. IR: (CH_2Cl_2) ν(C≡C) 2113 cm^{-1}. ^1H NMR: (δ, 300 MHz, $CDCl_3$); (0.49 (d, J_{HH} = 6 Hz, 3H), 0.58 (d, J_{HH} = 6 Hz, 3H), 0.76 (d, J_{HH} = 6 Hz, 3H), 0.95 (m), 1.30 (m), 1.60 (m), 1.95 (m), 2.78 (m), 3.59 (m), neomenthyl), (7.42 (m), 7.94 (m), 8.13 (m), Ph), 7.10 (d, J_{HH} = 16 Hz, 1H, H_{15}), 7.23 (d, J_{HH} = 16 Hz, 1H, H_{16}), 7.48 (d, J_{HH} = 8 Hz, 2H, H_4), 7.57 (d, J_{HH} = 9 Hz, 2H, H_{10}), 7.60 (d, J_{HH} = 8 Hz, 2H, H_5), 8.20 (d, J_{HH} = 9 Hz, 2H, H_{11}). ^{31}P NMR: (δ, 121 MHz, $CDCl_3$); 38.6. UV–vis: λ (nm) (ε (M^{-1} cm^{-1})) (thf): 388 (38 900), 302 (19 200). FAB MS; *m/z* (fragment, relative intensity): 1290 ([M + Au(nmdpp)]$^+$, 54), 845 ([Au(nmdpp)$_2$]$^+$, 94), 770 ([M + H]$^+$, 60), 521 ([M − C≡CC$_6$H$_4$CH=CHC$_6$H$_4$NO$_2$]$^+$, 40), 383 ([M − C≡CC$_6$H$_4$CH=CHC$_6$H$_4$NO$_2$ − neomenthyl + H]$^+$, 100), 305 ([M − C≡CC$_6$H$_4$CH=CHC$_6$H$_4$NO$_2$ − neomenthyl − Ph]$^+$, 23). Crystals of **5** suitable for X-ray diffraction analysis were grown by slow evaporation of a solution in dichloromethane.

3.2.6. Synthesis of Au((Z)-4,4′-C≡CC$_6$H$_4$CH=CHC$_6$H$_4$NO$_2$)(nmdpp) (6)

AuCl(nmdpp) (100 mg, 0.18 mmol), a trace of nmdpp oxide and (*Z*)-4,4′-HC≡CC$_6$H$_4$CH=CHC$_6$H$_4$NO$_2$ (50 mg, 0.20 mmol) were added to methanol (5 ml). A methanol solution of sodium methoxide (5 ml, 0.20 M) was added and the mixture was stirred at room temperature for 16 h after

which time a yellow solid had precipitated. Filtration afforded the product as a yellow microcrystalline powder (108 mg, 78%). Anal. Calc. for $C_{38}H_{39}AuNO_2P$: C 59.29, H 5.12, N 1.82%. Found: C 59.50, H 5.02, N 1.65%. IR: (CH_2Cl_2) ν(C≡C) 2114 cm^{-1}. ^1H NMR: (δ, 300 MHz, $CDCl_3$); (0.48 (d, J_{HH} = 6 Hz, 3H), 0.57 (d, J_{HH} = 6 Hz, 3H), 0.75 (d, J_{HH} = 6 Hz, 3H), 0.95 (m), 1.28 (m), 1.60 (m), 1.95 (m), 2.75 (m), 3.58 (m), neomenthyl), (7.41 (m), 7.93 (m), 8.10 (m), Ph), 6.55 (d, J_{HH} = 12 Hz, 1H, H_{15}), 6.76 (d, J_{HH} = 12 Hz, 1H, H_{16}), 7.10 (d, J_{HH} = 8 Hz, 2H, H_4), 7.36 (d, J_{HH} = 8 Hz, 2H, H_5), H_{10} is obscured, 8.04 (d, J_{HH} = 9 Hz, 2H, H_{11}). ^{31}P NMR: (δ, 121 MHz, $CDCl_3$); 38.6. UV–vis: λ (nm) (ε (M^{-1} cm^{-1})) (thf): 370 (15 500), 295 (30 800). FAB MS; *m/z* (fragment, relative intensity): 1290 ([M + Au(nmdpp)]$^+$, 20), 845 ([Au(nmdpp)$_2$]$^+$, 100), 770 ([M + H]$^+$, 22), 521 ([M − C≡CC_6H_4CH=CH$C_6H_4NO_2$]$^+$, 13), 383 ([M − C≡CC_6H_4CH=CH$C_6H_4NO_2$ − neomenthyl + H]$^+$, 45), 305 ([M − C≡CC_6H_4CH=CH$C_6H_4NO_2$ − neomenthyl − Ph]$^+$, 15).

3.2.7. Synthesis of Au(4,4′-C≡CC_6H_4C≡C$C_6H_4NO_2$)(nmdpp) (7)

AuCl(nmdpp) (52 mg, 0.09 mmol) and 4,4′-HC≡CC_6H_4C≡C$C_6H_4NO_2$ (30 mg, 0.12 mmol) and triphenylphosphine oxide (5 mg, 0.02 mmol) were added to methanol (15 ml) and dichloromethane (5 ml). A methanol solution of sodium methoxide (5 ml, 0.20 M) was added and the mixture was stirred at room temperature for 16 h. The dichloromethane was removed under reduced pressure and the mixture was filtered.

Concentration of the filtrate and addition of water (0.5 ml) precipitated the product as a yellow powder (51 mg, 71%). Anal. Calc. for $C_{38}H_{37}AuNO_2P$: C 59.45, H 4.98, N 1.82%. Found: C 59.53, H 4.73, N 1.85%. IR: (CH_2Cl_2) ν(C≡C) 2114 cm^{-1}. ^1H NMR: (δ, 300 MHz, $CDCl_3$); (0.49 (d, J_{HH} = 6 Hz, 3H), 0.58 (d, J_{HH} = 6 Hz, 3H), 0.77 (d, J_{HH} = 6 Hz, 3H), 0.95 (m), 1.30 (m), 1.60 (m), 1.95 (m), 2.77 (m), 3.59 (m), neomenthyl), (7.43 (m), 7.94 (m), 8.12 (m), Ph), H_4 is obscured, 7.55 (d, J_{HH} = 8 Hz, 2H, H_5), 7.64 (d, J_{HH} = 9 Hz, 2H, H_{10}), 8.20 (d, J_{HH} = 9 Hz, 2H, H_{11}). ^{31}P NMR: (δ, 121 MHz, $CDCl_3$); 38.6. UV–vis: λ (nm) (ε (M^{-1} cm^{-1})) (thf): 366 (34 600), 301 (29 300). FAB MS; *m/z* (fragment, relative intensity): 1288 ([M + Au(nmdpp)]$^+$, 42), 845 ([Au(nmdpp)$_2$]$^+$, 76), 768 ([M + H]$^+$, 21), 521 ([M − C≡CC_6H_4C≡C$C_6H_4NO_2$]$^+$, 16), 383 ([M − C≡CC_6H_4C≡C$C_6H_4NO_2$ − neomenthyl + H]$^+$, 100), 305 ([M − C≡CC_6H_4C≡C$C_6H_4NO_2$ − neomenthyl − Ph]$^+$, 14).

3.2.8. Synthesis of Au(4,4′-C≡CC_6H_4N=C$HC_6H_4NO_2$)(nmdpp) (8)

AuCl(nmdpp) (50 mg, 0.09 mmol), 4,4′-HC≡CC_6H_4N=C$HC_6H_4NO_2$ (25 mg, 0.10 mmol) and triphenylphosphine oxide (5 mg, 0.02 mmol) were added to methanol (15 ml). A methanol solution of sodium methoxide (5 ml, 0.20 M) was added and the mixture was stirred at room temperature for 16 h. The mixture was filtered and the filtrate concentrated under reduced pressure to afford the product as a yellow powder (37 mg, 53%). Anal. Calc. for $C_{37}H_{38}AuNO_2P$: C 57.66, H 4.98, N 3.64%. Found: C 57.49, H 4.68, N 3.49%. IR: (CH_2Cl_2) ν(C≡C) 2114 cm^{-1}. ^1H NMR: (δ, 300 MHz, $CDCl_3$); (0.49 (d, J_{HH} = 6 Hz, 3H), 0.58 (d, J_{HH} = 6 Hz, 3H), 0.77 (d, J_{HH} = 6 Hz, 3H), 0.95 (m), 1.30 (m), 1.60 (m), 1.95 (m), 2.77 (m), 3.59 (m), neomenthyl), (7.43 (m), 7.94 (m), 8.12 (m), Ph), 7.19 (d, J_{HH} = 8 Hz, 2H, H_4), 7.61 (d, J_{HH} = 8 Hz, 2H, H_5), 8.05 (d, J_{HH} = 9 Hz, 2H, H_{10}), 8.31 (d, J_{HH} = 9 Hz, 2H, H_{11}), 8.56 (1H, H_{16}). ^{31}P NMR: (δ, 121 MHz, $CDCl_3$); 38.6. UV–vis: λ (nm) (ε (M^{-1} cm^{-1})) (thf): 394 (20 300), 293 (31 300). FAB MS; *m/z* (fragment, relative intensity): 1292 ([M + Au(nmdpp)]$^+$, 100), 845 ([Au(nmdpp)$_2$]$^+$, 31), 771 ([M + H]$^+$, 46), 521 ([M − C≡CC_6H_4N=CH$C_6H_4NO_2$]$^+$, 19), 383 ([M − C≡CC_6H_4N=CH$C_6H_4NO_2$ − neomenthyl + H]$^+$, 70), 305 ([M − C≡CC_6H_4N=CH$C_6H_4NO_2$ − neomenthyl − Ph]$^+$, 16).

3.3. X-ray structure determinations

3.3.1. General considerations

Unique diffractometer data sets were obtained using the ω–2θ scan technique (graphite monochromated Mo Kα radiation; 0.71069 Å; $2\theta_{max}$ = 50.1°; 295 K for **2** and graphite monochromated Cu Kα radiation; 1.5418 Å; $2\theta_{max}$ = 120.2°; 295 K for **5**) and yielded N independent reflections, N_0 of these with $I \geq 3.00\sigma(I)$ being considered 'observed' and used in full matrix least squares refinement; an empirical psi-type absorption correction was applied in each case. Anisotropic thermal parameters were refined for the non-hydrogen atoms (**2**) or non-carbon or non-hydrogen atoms (**5**); (x, y, z, U_{iso})$_H$ were included constrained at estimated values, except for hydrogen atoms on the neomenthyl group in **5** which were omitted. Conventional residuals R and R_w on $|F|$ are given; the weighting function $w = 4F_o^2/\sigma^2(F_o^2)$ where $\sigma^2(F_o^2) = [S^2(C + 4B) + (pF_o^2)^2]/Lp^2$ (S is the scan rate, C is the peak count, B is the background count, p is the p factor determined experimentally from standard reflections) was employed. Computation used the teXsan package [29]. Specific data collection, solution and refinement parameters are given in Table 1. Pertinent results are given in the figures and tables. For **2**, tables of atomic coordinates and thermal parameters and complete lists of bond lengths and angles for non-hydrogen atoms have been deposited at the Cambridge Crystallographic Data Centre.

3.3.2. Unusual features / variations in procedure

Complex **2** refined satisfactorily. Complex **5** was refined in the centrosymmetric space group $P\bar{1}$ (two molecules in the asymmetric unit) with disorder and consequent bond and angle restraints in the neomenthyl groups. Attempts to refine the structure in the more 'sensible' (given the existence of optically pure chiral substituents) space group $P1$ (four molecules in the asymmetric unit) were unsuccessful. The unsatisfactory structural study does, however, establish conclusively the molecular disposition in the crystal lattice, including the antiparallel arrangement of neighbouring dipolar gold acetylides.

3.4. Powder measurements

Samples were ungraded microcrystalline powders placed in the circular cavity (10 mm diameter × 0.5 mm depth) of a microscope slide with a cover slip. Powder SHG efficiencies were measured using the Kurtz technique [25]. The fundamental output of a Q-switched Quanta-Ray GC-130 Nd:YAG laser was directed onto the sample (spot size ca. 5 mm; energy per pulse: up to 20 mJ). A collecting lens (orthogonally placed with respect to the fundamental beam) focused the backscattered second-harmonic light through an infrared absorbing filter and a 532 nm interference filter onto a photodiode detector, which was connected to an HP digital 54510A oscilloscope. Measurements thus made were compared with a urea powder sample.

Acknowledgements

We thank the Australian Research Council for support of this work. I.R.W. is the recipient of an Australian Postgraduate Research Award (Industry) and M.G.H. holds an ARC Australian Research Fellowship. Dr. S.B. Wild is thanked for the gift of some nmdpp and Mr. D. Bogsányi for obtaining the UV–visible spectra.

References

[1] I.R. Whittall, M.P. Cifuentes, M.G. Humphrey, B. Luther-Davies, M. Samoc, S. Houbrechts, A. Persoons, G.A. Heath, D. Bogsányi, D.C.R. Hockless, Organometallics, in press.
[2] I.R. Whittall, A.M. McDonagh, M.G. Humphrey, M. Samoc, Adv. Organomet. Chem. in press.
[3] S.R. Marder, in: D.W. Bruce, D. O'Hare (Eds.), Inorganic Materials, Wiley, Chichester, UK, 1992, p. 115.
[4] H.S. Nalwa, Appl. Organomet. Chem. 5 (1991) 349.
[5] N.J. Long, Angew. Chem. Int. Ed. Engl. 34 (1995) 21.
[6] I.R. Whittall, M.G. Humphrey, S. Houbrechts, A. Persoons, Organometallics 15 (1996) 1935.
[7] I.R. Whittall, M.G. Humphrey, S. Houbrechts, A. Persoons, D.C.R. Hockless, Organometallics, 15 (1996) 5738.
[8] I.R. Whittall, M.P. Cifuentes, M.G. Humphrey, B. Luther-Davies, M. Samoc, S. Houbrechts, A. Persoons, G.A. Heath, D.C.R. Hockless, submitted to J. Organomet. Chem.
[9] S. Houbrechts, K. Clays, A. Persoons, V. Cadierno, M.P. Gamasa, J. Gimeno, I.R. Whittall, M.G. Humphrey, Proc. SPIE-Int. Soc. Opt. Eng. 2852 (1996) 98.
[10] ZINDO User Guide, Biosym Technologies, San Diego, USA, 1994.
[11] I.R. Whittall, M.G. Humphrey, D.C.R. Hockless, B.W. Skelton, A.H. White, Organometallics 14 (1995) 3970.
[12] A.M. McDonagh, I.R. Whittall, M.G. Humphrey, B.W. Skelton, A.H. White, J. Organomet. Chem. 519 (1996) 229.
[13] A.M. McDonagh, I.R. Whittall, M.G. Humphrey, M.G. Humprey, B.W. Skelton, A.H. White, J. Organomet. Chem. 523 (1996) 33.
[14] I.R. Whittall, M.G. Humphrey, M. Samoc, J. Swiatkiewicz, B. Luther-Davies, Organometallics 14 (1995) 5493.
[15] A.M. McDonagh, M.P. Cifuentes, I.R. Whittall, M.G. Humphrey, M. Samoc, B. Luther-Davies, D.C.R. Hockless, J Organomet. Chem. 526 (1996) 99.
[16] I.R. Whittall, M.G. Humphrey, M. Samoc, B. Luther-Davies, Angew. Chem., Int. Ed. Engl. 36 (1997) 370.
[17] R. Uson, A. Laguna, I.J. Vicente, J. Organomet. Chem. 131 (1977) 471.
[18] M.I. Bruce, B.K. Nicholson, O. bin Shawkataly, Inorg. Synth. 26 (1989) 324.
[19] M.I. Bruce, E. Horn, J.G. Matisons, M.R. Snow, Aust. J. Chem. 37 (1984) 1163.
[20] R. Cross, M.F. Davidson, A.J. McLennan, J. Organomet. Chem. 265 (1984) C37.
[21] G. Jaouen, J.A.S. Howell, M.-C. Tirvengadum. P. McArdle, D. Cunningham, J. Organomet. Chem. 370 (1989) 51.
[22] (a) J.A.S. Howell, A.D. Squibb, A.G. Bell, P. McArdle, D. Cunningham, Z. Goldschmidt, H.E. Gottlieb, D. Hezroni-Langerman, R. Grée, Organometallics 13 (1994) 4336. (b) J.A.S. Howell, M.-C. Tirvengadum, A.D. Squibb, G. Walton, P. McArdle, D. Cunningham, J. Organomet. Chem. 347 (1988) C5. (c) J.A.S. Howell, A.D. Squibb, G. Walton, P. McArdle, D. Cunningham, J. Organomet. Chem. 319 (1987) C45. (d) J.A.S. Howell, M.G. Palin, M.-C. Tirvengadum, D. Cunningham, P. McArdle, Z. Goldschmidt, H.E. Gottlieb, J. Organomet. Chem. 413 (1991) 269. (e) A. Marcuzzi, A. Linden, D. Rentsch, W. von Phillipsborn, J. Organomet. Chem. 429 (1992) 87.
[23] (a) P. Salvadori, P. Pertici, F. Marchetti, R. Lazzaroni, G. Vitulli, M.A. Bennett, J. Organomet. Chem. 370 (1989) 155. (b) P. Pertici, E. Pitzalis, F. Marchetti, C. Rosini, P. Salvadori, M.A. Bennett, J. Organomet Chem. 466 (1994) 221.
[24] P. Gugger, S.O. Limmer, A.A. Watson, A.C. Willis, S.B. Wild, Inorg. Chem. 32 (1993) 5692.
[25] S.K. Kurtz, T.T. Perry, J. Appl. Phys. 39 (1968) 3798.
[26] J.D. Morrison, W.F. Masler, J. Org. Chem. 39 (1974) 270.
[27] S. Takahashi, Y. Kuroyama, K. Sonogashira, N. Hagihara, Synthesis (1980) 627.
[28] D.C.R. Hockless, I.R. Whittall, M.G. Humphrey, Acta Crystallogr. Sect. C: 52 (1996) 3222.
[29] teXsan: Single Crystal Structure Analysis Software, Version 1.6c, 1993, Molecular Structure Corporation, The Woodlands, TX, USA.